Journal of Telecommunication, Electronic and Computer Engineering
ISSN: 2180 – 1843 e-ISSN: 2289-8131 Vol. 14 No. 4
jtec.utem.edu.my

Electromagnetic Analysis of Periodic Iris-Fed Patch Antenna Array Using Fast and Efficient Hybrid Analytical Approach

M.Abdi, T. Aguili
Syscom Laboratory, National Engineering School of Tunis, Tunis El Manar University BP 37, le Belvédère, Tunisia
mariemahmedabdi@gmail.com

Article Info

Article history:
Received Sep 27th, 2022
Revised Oct 25th, 2022
Accepted Nov 25th, 2022

Index Terms:
MOM-GEC
Spectral decomposition
Antenna array
Mutual coupling

Abstract

Planar antenna arrays are renowned for their high directivity and ease of implementation, while offering the possibility of controlling the radiation pattern. However, the study of the electromagnetic aspect taking into account the coupling between the array's elements requires a memory space and a considerable calculation time. To overcome these drawbacks, a fast and rigorous full-wave numerical method for the electromagnetic analysis of a unidimensional periodic iris-fed patch antenna array has been proposed. The spatial electromagnetic calculation of a periodic structure of finite dimensions is reduced to a spectral calculation carried out on a single unit reference cell by applying periodicity conditions to it. The modeling of a unit cell is based on the MOM-GEC flexible formalism, which reduces the resolution of the electromagnetic problem to a simple manipulation of equivalent circuits. Firstly, a validation of the numerical approach took place through the verification of the boundary conditions applied to the current distribution. Next, the mutual coupling between the elements of the antenna array was calculated. Results were validated with those obtained with HFSS commercial software and they yield accurate and efficient solutions. Furthermore, a significant reduction of both memory storage requirement and computational time was observed.

I. INTRODUCTION

The use of waveguide as a source of excitation for a microstrip patch antenna through a coupling slot has been proposed by [1]. Eventually, this technique has been widely applied in communication systems [2,3] for several reasons, such as low losses, high accuracy of design and mechanical resistance. Therefore, the iris-fed antenna constitutes a prime candidate for exploration, and it is proposed to be set into a periodic unidimensional array for X-band communications.

Modeling the propagation of electromagnetic fields from a periodic antenna array requires rigorous modal analysis methods. Moreover, the interaction between the radiating elements in periodic antenna arrays leads to the existence of intercellular couplings, which change the radio electric characteristics of the antenna. The design of antenna arrays therefore, requires prior knowledge of the mutual coupling between the different radiating elements. There are several approaches to modeling periodic antenna array, namely the "Full-wave" approaches and the modular approaches.

Classic full-wave approaches, such as the Method of Moments and the Method of Finite Differences are precise, efficient and reliable methods. However, they are not suitable for large array. It is therefore necessary to focus on more developed full-wave approaches, such as the domain decomposition method (DDM) [4] and the multilevel fast multipole method (MLFMM) [5]. These methods are dedicated to analyzing large periodic structures. Admittedly, they require expertise in the use of simulation software by conducting an advanced convergence study of the cases studied.

The modular approaches consist in individually characterizing one or a few cells of the antenna array to deduce the total radiation of the array. Several modular approaches have been proposed for modeling the elementary cell, namely the isolated cell approach, the surrounded cell approach and the Scale Changing Technique (SCT) method [6]. The isolated cell approach neglects the mutual couplings between the lattice elements; hence, it does not seem to be an interesting approach for the study of large periodic lattices behavior. The surrounded cell approach takes into account the real couplings between network elements. The disadvantage of this method is that the number of considered adjacent cells depends on the nature of the coupling: If it is a high number, it results in a very long calculation time. The (SCT) presents an interesting alternative, but its implementation is complex. Most of these methods are not easy to apply on antenna arrays with a large number of radiating elements. Moreover, the infinity with the periodic character of the array makes the problem more complicated.

As a consequence, this work tends to overcome the limitations of the classic full-wave approaches by using a rigorous full-wave numerical method for the calculation of the mutual coupling between elements in a unidimensional periodic iris-fed patch antenna array. In fact, the full-wave method that comprises a hybridization of the MOM-GEC method and a unit-cell spectral decomposition approach is described in the next section.

This paper is divided as follows. In section II, the

methodology problem statement is explained. In section III, the mathematical formulation based the hybridized MOM-GEC combined with the unit-cell spectral decomposition approach is applied to a periodic five-element iris-fed antenna array. The numerical resolution is presented along with the results in section IV.

II. METHODOLOGY PROBLEM STATEMENT

Although researches related to the analysis of periodic antenna array based on Floquet theory are still in progress, it is proposed to be adopted as an approach for the electromagnetic modelling of the periodic antenna array. In fact, Floquet's approach [7], also called infinite periodic approach, advocates that all the cells of the periodic array must be identical and reproduced to infinity according to the directions of the periodicity of the antenna. The excitations, which are applied to them must also be of identical intensities and can undergo a constant phase shift between two adjacent cells consistent with one periodic direction.

The application of the periodicity conditions results in the reduction of the spatial electromagnetic calculation of a periodic structure of infinite dimensions to a spectral calculation carried out on a single reference cell. These boundary conditions make it possible to obtain the behavior of the latter, when a uniform and infinite environment surrounds it.

The physical reality of the applications used cannot include an infinity of patterns. In the literature, various approaches have been adopted to study a network with a finite number of patterns, namely the approaches of: Roederer, Ishimaru, Skrivervik and Mosig, Parfitt, etc. Without the need of the Green function formulation, this work proposed to use the method of spectral modal decomposition of the centered reference source situated in a finite periodic antenna array with odd number of elements [8-9] (see Figure. 1(a)).

The modeling of the unit cell is made by using MOM-GEC flexible formalism, which reduces the resolution of the electromagnetic problem in a simple handling of the Generalized Equivalent Circuits (GEC). The method of moments (MOM), considered as one of the most efficient integral methods, is hybridized with the Generalized Equivalent Circuits Method (GEC) to reduce the resolution of Maxwell's equations by describing the boundary conditions of the structure through a simple equivalent electrical circuit [10]. To treat the structure simpler and more understandable, auxiliary sources (AS) intervene in the extraction of the generalized equivalent circuit to ensure the interconnection of the exciter waveguide with the microstrip patch antenna. Thereby, the MOM-GEC method combined with the unit-cell spectral decomposition approach is adopted for the calculation of the mutual coupling between elements in a unidimensional periodic millimeter-wave patch antenna array.

The unit-cell antenna consisting of an iris-fed microstrip patch antenna is illustrated in Figure 1(b). The structure is formed by a dielectric substrate situated between a patch and a feeder waveguide. The feeder waveguide consists of an iris that terminates a WR90 rectangular waveguide, leading to the electromagnetic radiation to be oriented to the patch through the aperture. The GEC of the antenna is presented in Figure 1(c). The flowchart of MOM-GEC hybridized with the unit-cell spectral decomposition approach is illustrated in Figure 2.

III. PROBLEM FORMULATION

This section presents the steps mentioned in Figure 2.

A. GEC of unit reference cell

The antenna is composed of an iris excited by the fundamental TE_{10} mode and a microstrip patch antenna excited by the TEM mode. Each virtual waveguide is defined by the electrical periodic walls (EPEP) and is associated with a modal base function $f_{mn,\alpha}$, where m and n are integers related to the mode (see Figure 3).

Noting that: $J_{01,\alpha}$ is the real current source of the unit cell expressed according to the amplitude $I_{01,\alpha}$ and the fundamental mode $f_{0,\alpha}$ of the modal base function $f_{mn,\alpha}$; $E_{01,\alpha}$ is the real field source E_{01} expressed according the amplitude $V_{01,\alpha}$ and the fundamental mode $f_{0,\alpha}$ of the modal base function $f_{mn,\alpha}$; $J_{02,\alpha}$ is the auxiliary current source expressed according to the amplitude $I_{02,\alpha}$ and the fundamental mode ${f_{0,\alpha}}'$of the modal base function ${f'}_{mn,\alpha}$; $E_{02,\alpha}$ is the auxiliary electric field source expressed according to the amplitude $V_{02,\alpha}$ and the fundamental mode ${f_{0,\alpha}}'$of the modal base function ${f'}_{mn,\alpha}$; $E_{e_{1,\alpha}}$ and $E_{e_2,\alpha}$ are the virtual electric fields and expressed in terms of test function $(g_{1,\alpha_p})_{p=1,..,N_{test}}$ and weighting coefficients $x_{p,\alpha}$; $\widehat{Y_{ev1,\alpha}}$ is the admittance of the modal source representing the evanescent modes at the level of discontinuity D_1 of the exciter waveguide, which is associated with the modal base function $(f_{mn,\alpha})_{(m,n)=\{1,..,N_b{}^2\}}$; $\widehat{Y_{ev2,\alpha}}$ is the admittance of the modal source representing the evanescent modes at the level of discontinuity D_2 of the exciter waveguide, which is associated with the modal base function $({f'}_{mn,\alpha})_{(m,n)=\{1,..,N_b{}^2\}}$; $\widehat{Y_{11,\alpha}}$ is the input admittance and $\widehat{Y_{12,\alpha}}$ the inverse transfer admittance of quadrupole associated with the modal base function $({f'}_{mn,\alpha})_{(m,n)=\{1,..,N_b{}^2\}}$; E_α is the unit cell virtual electric field; $J_{s,\alpha}$ is the unit cell virtual current distribution expressed in terms of test function $(g_{2,\alpha_p})_{p=1,..,Ntest}$ and weighting coefficients $x_{p,\alpha}$; ; $\widehat{Y_{th,\alpha}}$ is admittance of the dielectric layer; $\widehat{Y_{s,\alpha}}$ is admittance from the vacuum brought to the surface of the dielectric D_3.

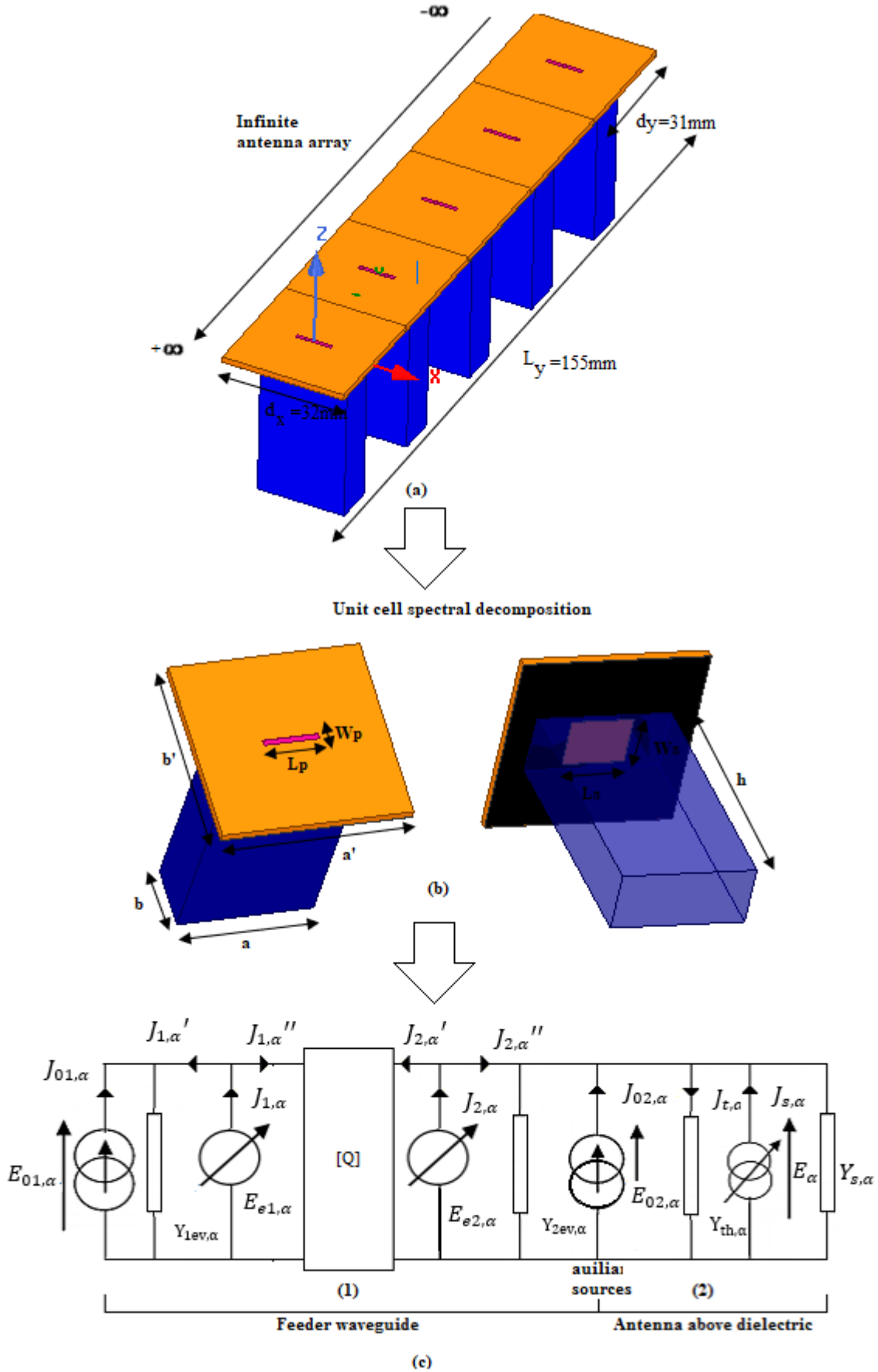

Figure 1.(a) Infinite unidimensional periodic iris-fed microstrip patch antenna array presentation with Floquet theory (b) unit cell (c) GEC of the unit cell: a=22.86, b=10.16, h=41.5, a′ =32, b′ =31, W_p=0.93, L_p=8, W_s=8.28, L_s=10.62, t_1(substrate thickness) = 1.5, t (patch thickness =ground thickness) =0.025, (all dimensions in millimeter),$\varepsilon r_{(FR4)}$ =4.4

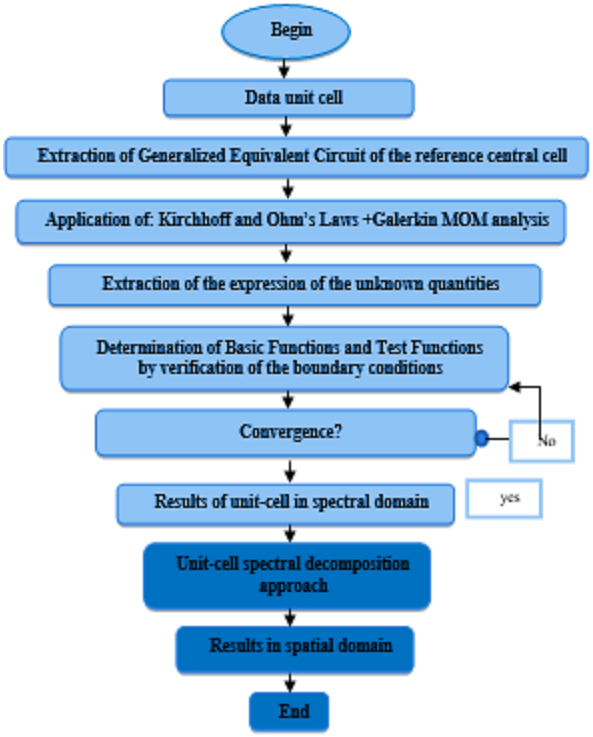

Figure 2. Flowchart of MOM-GEC hybridized with unit-cell spectral decomposition approach

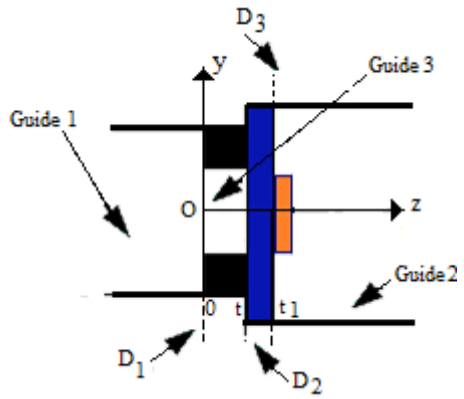

Figure 3. Unit reference shielded in rectangular waveguide defined by electrical periodic walls (EPEP) on all faces with discontinuity planes

Real sources, such as current density or electric field are expressed as follows [11]:

$$J_{01,\alpha} = I_{01,\alpha} f_{0,\alpha} \tag{1}$$

$$E_{01,\alpha} = V_{01,\alpha} f_{0,\alpha} + \sum_{mn,\alpha}^{N_b} V_{01,\alpha} f_{mn,\alpha} \tag{2}$$

$$J_{02,\alpha} = I_{02,\alpha} f_{0,\alpha}' \tag{3}$$

$$E_{02,\alpha} = V_{02,\alpha} f_{0,\alpha}' + \sum_{mn,\alpha}^{N_b} V_{02,\alpha} f_{mn,\alpha}' \tag{4}$$

The virtual or adjustable sources defined by the discontinuity surfaces of current density or electric field type represents the test functions and they are expressed as follows [12]:

$$E_{e_1,\alpha} = \sum_{p,\alpha}^{N_{test}} x_{p,\alpha} g_{1,\alpha p} \tag{5}$$

$$J_{s,\alpha} = \sum_{p,\alpha}^{N_{test}} x_{p,\alpha} g_{2,\alpha p} \tag{6}$$

The admittance operators that describe the behaviour of the guides are expressed as follows [13]:

$$\hat{Y}_{ev1,\alpha} = \sum_{\alpha=TE,TM} \left| \overset{\alpha}{f}_{mn,\alpha} \right\rangle \overset{\alpha}{y}_{ev1,\alpha} \left\langle \overset{\alpha}{f}_{mn,\alpha} \right| \tag{7}$$

$$\hat{Y}_{ev2/11/12/th/s,\alpha} = \sum_{\alpha=TE,TM} \left| \overset{\alpha}{f}_{mn,\alpha}' \right\rangle \overset{\alpha}{y}_{ev2/11/12/th/s,\alpha} \left\langle \overset{\alpha}{f}_{mn,\alpha}' \right| \tag{8}$$

B. Galerkin method application

The writing of the cancellation of the dual quantities of the virtual sources in their domain of definition is solved by the method of Galerkin [14]. In fact, Galerkin method application allows to solve electromagnetic equations expressed b (V, I) physical scales instead of using (E, J) physical scales. Therefore, it leads to the following matrix systems;

On side (1):

$$\begin{pmatrix} V_{01,\alpha} \\ V_{02} \end{pmatrix} = \begin{pmatrix} [A_\alpha]^t [D_{1\alpha}]^{-1} [A_\alpha] & [B_\alpha]^t [C_\alpha]^{-1} [A_\alpha] \\ [A_\alpha]^t [C_\alpha]^{-1} [B_\alpha] & [B_\alpha]^t [D_{2\alpha}]^{-1} [B_\alpha] \end{pmatrix} \begin{pmatrix} I_{01,\alpha} \\ I_{02,\alpha} \end{pmatrix} \tag{9}$$

On side (2):

$$\begin{pmatrix} V_{02,\alpha} \\ [0] \end{pmatrix} = \begin{pmatrix} [A_{0,\alpha}] & [A_{1,\alpha}]^t \\ [A_{1,\alpha}] & [C_{1,\alpha}] \end{pmatrix} \begin{pmatrix} I_{02,\alpha} \\ [X_\alpha] \end{pmatrix} \tag{10}$$

The vector ponderation is expressed by:

$$[X_\alpha] = \sum_{p\alpha}^{N_{test}} x_{p\alpha} \tag{11}$$

The first excitation vector on side (1) is defined by:

$$[A_\alpha] = \langle g_{1,\alpha p}, f_{0,\alpha} \rangle \tag{12}$$

The second excitation vector on side (1) is defined by:

$$[B_\alpha] = \langle g_{1,\alpha p}, f_{0,\alpha}' \rangle \tag{13}$$

The first impedance matrix on side (1) is expressed by:

$$[C_\alpha] = \langle g_{1,\alpha p}, \hat{Y}_{12,\alpha} g_{1\alpha q} \rangle \tag{14}$$

The second impedance matrix on side (1) is expressed by:

$$[D_{1,\alpha}] = \langle g_{1\alpha p}, (\hat{Y}_{ev_1,\alpha} + \hat{Y}_{11,\alpha}) g_{1q,\alpha} \rangle \tag{15}$$

The third impedance matrix on side (1) is expressed by:

$$[D_{2,\alpha}] = \langle g_{1\alpha p}, (\hat{Y}_{ev_2,\alpha} + \hat{Y}_{11,\alpha}) g_{1,\alpha q} \rangle \tag{16}$$

The excitation vector on side (2) is defined by:

$$[A_{1,\alpha}] = \langle g_{2,\alpha p}, \hat{Y}_{t_2,\alpha} f_{0,\alpha}' \rangle \tag{17}$$

The impedance matrix, which defines the coupling between *p* and *q* dielectric elements.

$$\left[C_{1,\alpha}\right] = y_{t_2,\alpha}^{-1} \sum_{mn}^{N_b} \langle g_{2,\alpha_p}, f_{mn,\alpha}' \rangle \langle f_{mn,\alpha}', g_{2,\alpha_q} \rangle \quad (18)$$

$$\left[A_{0,\alpha}\right] = \langle f_{0,\alpha}, \hat{Y}_{t_2}^{-1} f_{0,\alpha}' \rangle \quad (19)$$

C. Resolution of system matrix

The input impedance is deduced from equation (9) and expressed by:

$$Z_{in,\alpha} = [A_\alpha]^t [D_{1,\alpha}]^{-1} [A_\alpha] - \frac{[A_\alpha]^t [C_\alpha]^{-1} [B_\alpha] . [B_\alpha]^t [C_\alpha]^{-1} [A_\alpha]}{[B_\alpha]^t [D_{2,\alpha}]^{-1} [B_\alpha] - [B_\alpha]^t [C_\alpha]^{-1} [A_\alpha]} \quad (20)$$

The reflexion coefficient of unit reference cell is expressed by:

$$S_{11,\alpha} = \frac{Z_{in,\alpha} - Z_{0,\alpha}}{Z_{in,\alpha} + Z_{0,\alpha}} \quad (21)$$

The filed $E_{t\alpha}$ and the current field $J_{t\alpha}$ break down over the mode into a forward wave in $e^{-\gamma_{mn} z}$.

The current field $J_{t,\alpha}$ of unit central cell is expressed by:

$$J_{t,\alpha} = \left(\sum_{mn}^{N_b} \sum_{p_{,\alpha}=1}^{N_{test}} X_\alpha \langle f_{mn,\alpha}, g_{2,\alpha_p} \rangle f_{mn,\alpha} e^{-\gamma_{mn} z}\right) + \sum_{mn}^{N_b} \langle f_{mn,\alpha}, f_{01\alpha} \rangle f_{mn,\alpha} . I_{01\alpha} \quad (22)$$

The electric field $E_{t\alpha}$ of unit reference cell is expressed by:

$$E_{t\alpha} = \hat{Y}_{t_2\alpha}^{-1} J_{t\alpha} \quad (23)$$

D. Unit-cell spectral decomposition approach

Consider a 1-D antenna array along (Ox) composed by N_y identical cells, d_y periodically reproduced along (Oy) direction is described in Figure 4.

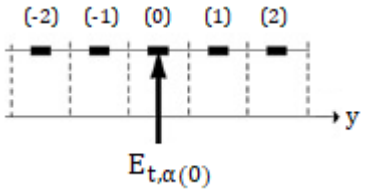

Figure 4. 1-D antenna array along (Oy) composed by five identical cells, d_y periodically reproduced along (Oy) direction and positioned according k={−2, −1,0,1,2}

To determine the spatial electric field on any elements of coordinates rd_x from the origin in an infinite antenna array with a phase shift of α between consecutive elements, it suffices to apply the following relations (24) [15-16]:

$$E(rd_y) = \frac{d_y}{2\pi} \int_{-\frac{\pi}{d_y}}^{\frac{\pi}{d_y}} E_{t,\alpha(0)}(x) e^{j^{\alpha r d_y}} d\alpha \quad (24)$$

We note that $E_{t,\alpha(0)}(y)$ is the spectral electric field of the reference central cell. The response of the method still provides us $J_{t,\alpha(0)}(y)$ with the spectral current on the unit central cell.

All the elements are included in one main period of the guide with L_y which delimits the overall structure. Thus, the discretization of spectral modes can be obtained by relying on a correspondence relationship (25) between the phase domain and the space of the patterns' positions in a finite lattice to ensure the discretization of the mode α [17]:

$$\begin{cases} 2\pi \rightarrow L_y \\ \alpha_p \rightarrow k \end{cases} \quad (25)$$

$$\alpha_k = \frac{2\pi k}{L_y} \text{ with } -\frac{N_y}{2} \leq k \leq \frac{N_y}{2} - 1 \quad (26)$$

The total electric field in the spatial domain on any elements are calculated by equations (27):

$$E_t(rd_y) = \frac{1}{N_y} \sum_{k=-\frac{N_y}{2}}^{\frac{N_y}{2}-1} E_{t,\alpha_k(0)} e^{j^{\frac{2\pi k}{L_y} rd_y}} \quad (27)$$

By applying the principles of FFT, the calculation of the mutual impedance and the scattering parameter between two elements of coordinates id_y and jd_y in the spatial domain are respectively defined in (28) and (29):

$$[Z_{i,j}] = TF^{-1} [Z_{\alpha_k}] TF \quad (28)$$

$$[S_{i,j}] = TF^{-1} [S_{\alpha_k}] TF \quad (29)$$

Noting that Z_{α_k} and S_{α_k} are respectively, the diagonal operator of input impedance and the scattering parameter related to spectral mode.

IV. RESULTS AND DISCUSSION

A. Study of convergence

The first step lies in determining the number of test functions and the number of base functions. Convergence indeed applies to one of the parameters of the antenna, namely, :the distribution of the current. The current becomes stable for N_{test}=11 and N_b=300, beyond these values, it remains unchangeable as illustrated in Figure 5. Therefore, these two values will be considered in the rest of the work.

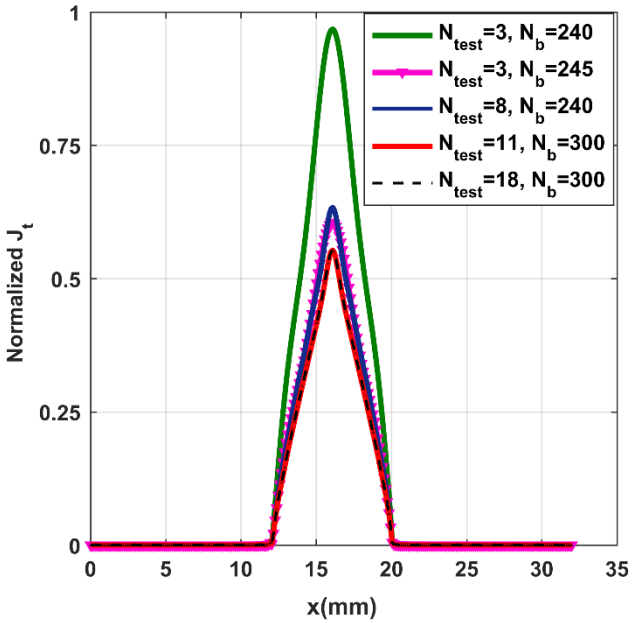

Figure 5. Normalized current distribution of the unit reference cell for different test functions and basic functions numbers.

B. Validation of MOM-GEC formulation

The current distribution of the unit reference cell is illustrated in Figure 6. It is regarded as the validation of the numerical method MOM-GEC applied on the cell of reference as it checks well the boundary conditions.

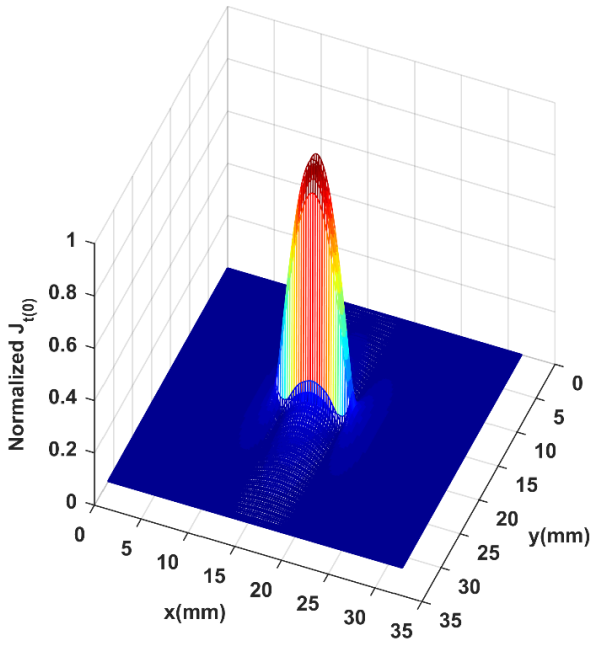

Figure 6. Normalized current distribution of the unit reference cell obtained at convergence for N_{test}=11 and N_b=300

The measured results of the reference cell are provided for the input matching (S11) due to the limitation of the measurement facilities. Figure 7 and Figure 8 shows the reference cell fabrication and the measurement set-up respectively. The reference cell is excited through iris by a rectangular waveguide of the Oritel TGN R100/WR90 type with 22.86mm×10.16mm×41.5mm dimension. In addition, the extended wall dimension is 56.5mm ×53mm.

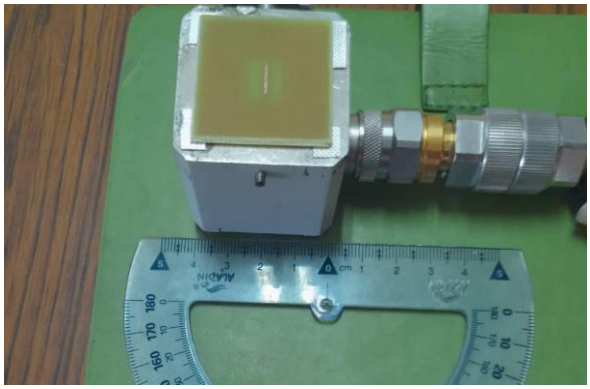

Figure 7. Fabricated unit reference cell: Microstrip patch antenna excited through iris by a rectangular waveguide

Figure 8. Coefficient reflection measurement of a fabricated unit reference cell: Microstrip patch antenna excited through iris.

The antenna reflection coefficient using MOM-GEC code and HFSS simulator is shown in Figure 9. The results are in good agreement with a small difference due to the different techniques used by each method.

The measured reference unit cell reflection coefficient is in good agreement with that obtained with the MOM-GEC method as illustrated in Figure 10. A small difference stands out since the effect of the connector was not taken into consideration during the numerical modelling.

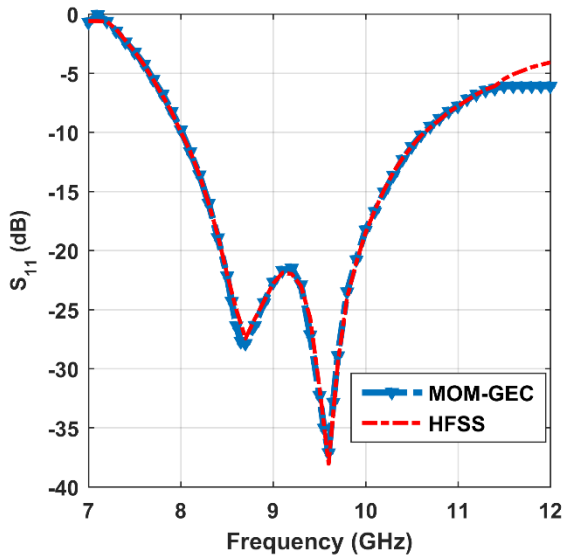

Fig. 9. Antenna reflection coefficient using MOM-GEC code and HFSS simulator

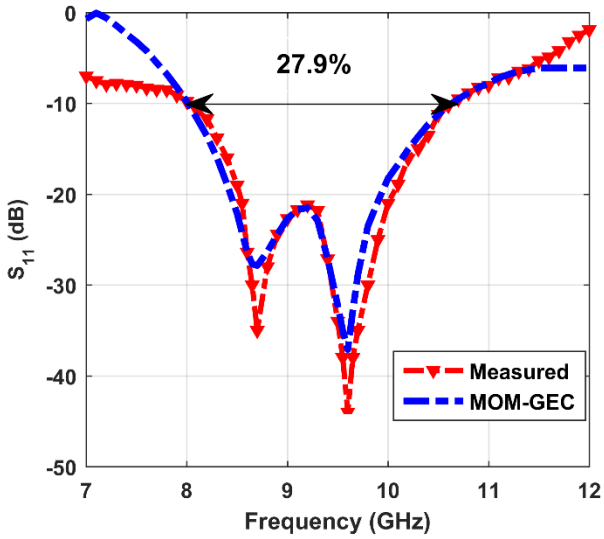

Fig. 10. Antenna reflection coefficient measured and using MOM-GEC code.

C. Validation of MOM-GEC-AS formulation with unit-cell spectral decomposition approach

In this section, we considered that the unit cell is excited by the internal waveguide with 22.86mm×10.16mm×41.5mm dimension. The extended walls were not taken into consideration for the antennas to be arranged on adjacent dielectrics.

The current distribution of the antenna array is illustrated in Figure 11. This is regarded as a validation of the numerical method MOM-GEC as it checks well the boundary conditions and

D. Mutual coupling calculation

Table 1 presents the mutual coupling parameter calculation between the array's elements based on the MOM-GEC formulation hybridized with the unit-cell spectral decomposition approach. Table 2 presents the mutual coupling parameter calculation between array's elements based HFSS simulator. The results are extracted at the resonant frequency fr=8.7GHz. In fact, they have a slight difference, which does not contradict the good agreement.

Table 1
Mutual coupling parameter calculation between array's elements based on the MOM-GEC formulation hybridized with unit-cell spectral decomposition approach

Position k	-2	-1	0	1	2
-2	-27.5	-22.37	-26.88	-26.88	-22.37
-1	-22.37	-27.5	-22.37	-26.88	-26.88
0	-26.88	-22.37	-27.5	-22.37	-26.88
1	-26.88	-26.88	-22.37	-27.5	-22.37
2	-22.37	-26.88	-26.88	-22.37	-27.5

Table 2
Mutual coupling parameter calculation between array's elements based HFSS simulator

Position k	-2	-1	0	1	2
-2	-26.3	-21.93	-25.9	-25.9	-21.93
-1	-21.93	-26.3	-21.93	-25.9	-25.9
0	-25.9	-21.93	-26.3	-21.93	-25.9
1	-25.9	-25.9	-21.93	-26.3	-21.93
2	-21.93	-25.9	-25.9	-21.93	-26.3

From the predicted mutual coupling values shown in Table 1 and Table 2, it can be inferred that the antennas are strongly decoupled, which confirms that the surface waves are not excited. Therefore, the use of techniques for minimizing the coupling effect in unnecessary.

In fact, the results validate the numerical calculation since the antennas are spaced by a distance of $\frac{\lambda}{2}$.

E. CPU time and memory storage

This section presents an evaluation of the formulation by spectral decomposition compared to the spatial formulation by the HFSS simulator in terms of computation and memory space. The CPU time and the memory storage required for the calculation of the mutual coupling parameters in function of antenna array's elements are illustrated in Figure 12 and Figure 13 respectively.

The mathematical complexity of the electromagnetic problem depends on the number of unknowns. Therefore, the CPU time and the memory storage required by a computer to solve a problem is expressed as a function of unknown numbers of the problem.

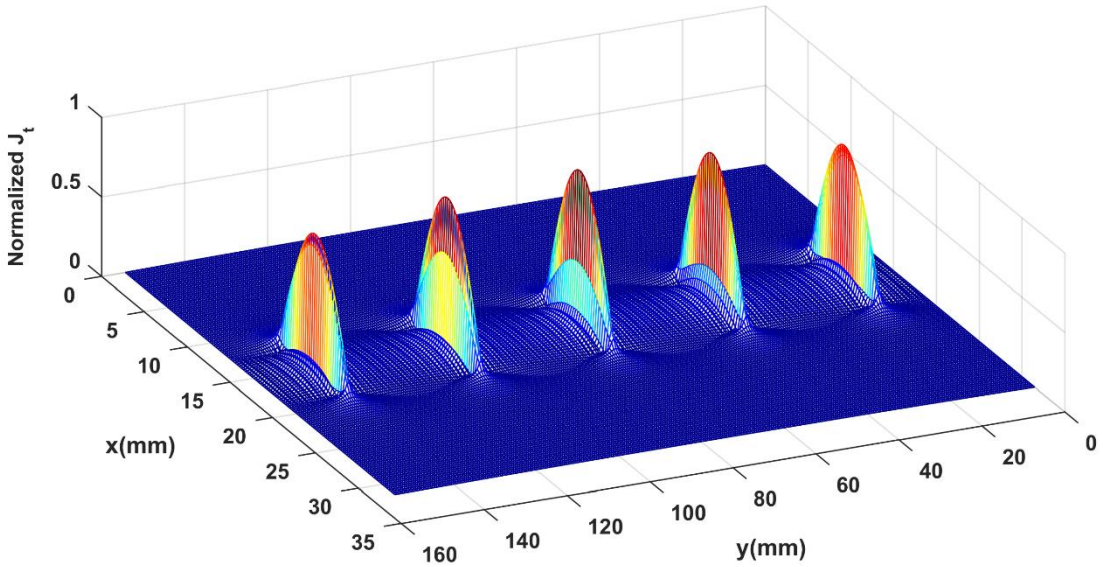

Figure. 11. Normalized current distribution of 1-D antenna array composed by five identical cells, d_y periodically reproduced along (Oy) direction and positioned according k={−2, −1,0,1,2} for L_x=32mm and L_y=155mm

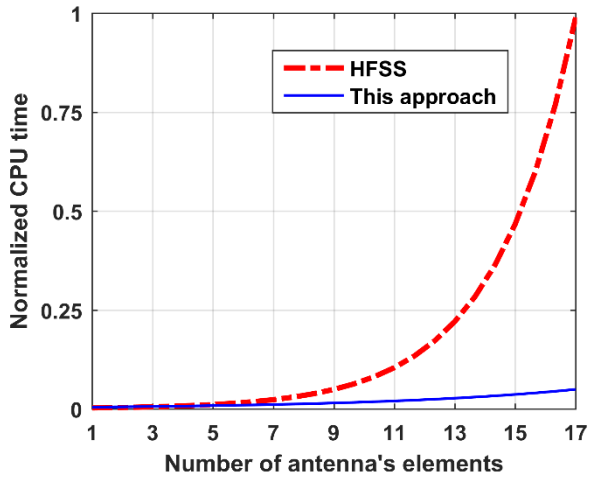

Fig. 12. CPU time required by using MOM-GEC code and HFSS simulator in function of antenna's elements for mutual coupling calculation

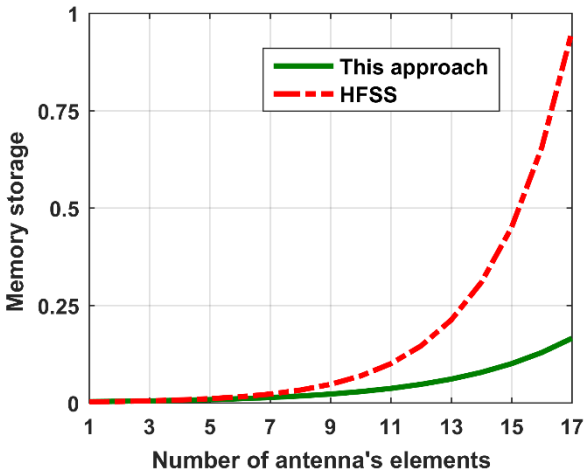

Fig. 13. Normalized memory storage required by using MOM-GEC code and HFSS simulator in function of antenna's elements for mutual coupling calculation

The Ansys HFSS calculator is essentially based on the finite element method, thus requiring a 3D mesh. When calculating the mutual coupling parameters, the HFSS simulator requires a matrix inversion (P × P), knowing that P is the number of test functions. In fact, the storage memory and the number of operations of the conventional HFSS simulator depends on P as [18]:

$$\text{Storage} \approx O(P^2) \tag{30}$$

$$\text{Operations number} \approx O(P^3) \tag{31}$$

Indeed, the total time required by the spatial formulation T_{HFSS} to calculate the impedance matrix is expressed as follows [19]:

$$T_{HFSS} = (\text{N} \times \text{P})^2 T_m + T_s \tag{32}$$

The total time required using the spectral formulation T_{spect} is expressed as follows:

$$T_{spect} = N.P^2.T_m + T_s \tag{33}$$

Noting that:

T_s is the necessary time required by a computer for calculating the matrix filling.

N^2: Elements of matrix resulted of N iterations.

T_m is the evaluation time of the multiplication operation required by a computer.

When the number of elements is limited, the difference between the two techniques in terms of computation time and memory space is not significant. Beyond seven elements, the difference between the two techniques becomes remarkable.

By application of the HFSS simulator, the calculation time as well as the required memory resources increase exponentially according to the number of network elements. This is explained by the fact that the number of unknowns and the number of operations of the problem is amplified when the number of network elements increases.

By applying the hybridized MOM-GEC formulation with spectral decomposition approach, the 3D investigation problem is converted to a 2D investigation problem. As a result, the number of operations is reduced and the calculation time as well as the memory resources are reduced

considerably compared to those obtained by applying a spatial formulation.

V. CONCLUSION

This work presents a new approach for calculating the mutual coupling between the elements of a five-element antenna array. This approach is based on the hybridization of the MOM-GEC method and the unit cell decomposition approach. A validation of the numerical approach was carried out by checking the boundary conditions on the current distribution of the central cell as well as the entire antenna array. Then, a calculation of the mutual coupling parameters was performed and compared to that obtained with HFSS simulator; the results are in good agreement. Moreover, a gain in terms of calculation time and memory space has been achieved. Hence, there is an interest of this approach in the analysis of antenna arrays with a large number of elements.

REFERENCES

[1] M. Kanda, D. Chang and D. Greenlee, "The Characteristics of Iris-Fed Millimeter-Wave Rectangular Microstrip Patch Antennas," IEEE Transactions on Electromagnetic Compatibility, vol. EMC-27, pp. 212–220, Nov. 1985.

[2] K. Wong, H. Chang, C. Wang and S. Wang, "Very-Low-Profile Grounded Coplanar Waveguide-Fed Dual-Band WLAN Slot Antenna for On-Body Antenna Application," IEEE Antennas and Wireless Propagation Letters, vol. 19, pp. 213–217, Dec. 2019.

[3] P. Liu, G. Frølund Pedersen and S. Zhang, "Wideband Slot Array Antenna Fed by Open-Ended Rectangular Waveguide at W-Band," IEEE Antennas and Wireless Propagation Letters, vol. 21, pp. 666–670, Apr. 2021.

[4] A. Barka; A. Jouadé and D. Jacquinot, "Simulation of Active Reflection Coefficient Phenomena of Large Antenna Array Using FEM Domain Decomposition Methods," IEEE Antennas and Wireless Propagation Letters, vol. 19, pp. 1789-1792, Oct. 2020.

[5] G. Karagounis, D. Zutter and D. Vande Ginste, "A Hybrid MLFMM–UTD Method for the Solution of Very Large 2-D Electromagnetic Problems," IEEE Transactions on Antennas and Propagation, vol. 64, pp. 224-234, Jun. 2016.

[6] F. Khalil, A. Rashid, H. Aubert; F. Coccetti, R. Plana, C.-J. Barrios-Hernandez and Y. Denneulin, "Application of Scale Changing Technique - grid computing to the electromagnetic simulation of reflectarrays," in *IEEE Antennas and Propagation Society International Symposium*, USA, 2009.

[7] B. Hamdi and T. Aguili, "Spectral Floquet analysis devoted to meta-surface applied for 5G and planned 6G antenna designs," in *International Symposium on Antenna Technology and Applied Electromagnetics (ANTEM)*, Canada, 2021.

[8] M. Zahéra and H. Baudrand, "Bi-dimensional bi-periodic centred-fed microstrip leaky-wave antenna analysis by a source modal decomposition in spectral domain," IET Microwaves Antennas & Propagation, vol. 3, no. 7, pp. 1141-1149, 2009.

[9] T. Lonsky, P. Hazdra and J. Kracek, "Modal decomposition for arbitrary dipole array," in *Conference on Microwave Techniques (COMITE)*, Czech Republic, 2017.

[10] M. Hajji, M. Aidi, H. Krraoui, and T. Aguili, "Hybridization of Generalized PO and MoM -GEC Method for Electromagnetic Study of Complex Structures: Application to Reflectarrays," Progress in Electromagnetics Research M, vol. 45, pp. 35-49, 2016.

[11] H. Baudrand, "Introduction au calcul des éléments de circuits passifs en hyperfréquences," Cépaduès éditions, Sept, 2021.

[12] B. Hamdi and T. Aguili, "Multiscale Auxiliary Sources for Modeling Microwave Components," Recent Microwave Technologies, March. 2021.

[13] H. Baudrand and D. Bajon, "Equivalent circuit representation for integral formulations of electromagnetic problems," International Journal of Numerical Modelling: Electronic Networks, Devices and Fields, vol. 15, pp. 23-57, 2002.

[14] X. Li, L. Xu, Z. Yang and B. Li, "The PML Boundary Application in the Implicit Hybridizability Discontinuous Galerkin Time-Domain Method for Waveguides, IEEE Microwave and Wireless Components Letters, vol. 31, no. 4, pp. 337-340, 2021.

[15] X.Z. Xiong, L. Meng, L. J. Jiang and W. Sha, "A New Efficient Method for Analysis of Finite Periodic Structures," *USNC-URSI Radio Science Meeting*, USA, 2014.

[16] A. Motevasselian, A. Ellgardt and B. L. G. Jonsson, "A New Efficient Method for Analysis of Finite Periodic Structures," *URSI General Assembly and Scientific Symposium*, Turkey, 2011.

[17] J. I. Echeveste, D. Tihon, M. Dubois, R. Abdeddaim; S. Enoch and C. Crae, "Efficient and full-wave electromagnetic analysis of MRI antennas using the array scanning method," *European Conference on Antennas and Propagation*, London, 2018.

[18] A. Khaled, D. Omri and T. Aguili, "A novel space hybrid meshing technique combined with Laguerre polynomial to solve TD-EFIE," Journal of Electromagnetic Waves and Applications, vol. 35, no. 12, pp. 1-21, Jan. 2021.

[19] D. Omri, M. Aidi and T. Aguili, "A comparison of three temporal basis functions for the time-domain method of moments (TD-MoM)," Journal of Computational Electronics, vol. 19, no. 12, pp. 750-758. 2020.